

Cite this: *Analyst*, 2013, **138**, 4542

Selective solid-phase extraction of naproxen drug from human urine samples using molecularly imprinted polymer-coated magnetic multi-walled carbon nanotubes prior to its spectrofluorometric determination

Tayyeb Madrakian,* Mazaher Ahmadi, Abbas Afkhami and Mohammad Soleimani

A drug imprinted polymer based on suspension polymerization on magnetic multi-walled carbon nanotubes (MIPMCNTs) was prepared with a synthesized amidoamine as the functional monomer, ethylene glycol dimethacrylate as the cross-linker, naproxen (NAP) as the template and ammonium persulfate as the initiator. The MIPMCNTs were characterized by TEM, FT-IR and XRD measurements. The prepared magnetic adsorbent can be well dispersed in aqueous media and can be easily separated magnetically from the medium after loading with NAP. All the aspects influencing the adsorption (extraction time, adsorbent dosage and pH) and desorption (desorption time and desorption solvent) of the analyte on the MIPMCNTs have been investigated. The extracted NAP could be easily desorbed with a mixture of methanol/sodium hydroxide aqueous solution and determined spectrofluorometrically at $\lambda_{em} = 353$ nm ($\lambda_{ex} = 271$ nm). A linear dynamic range was established from 4.0 to 40.0 ng mL⁻¹ of NAP and the limit of detection (LOD) was found to be 2.0 ng mL⁻¹. In addition, the equilibrium adsorption data of NAP by imprinted polymer were analyzed by Langmuir and Freundlich isotherm models. The developed method was utilized for the determination of NAP in human urine samples with satisfactory results.

Received 6th April 2013

Accepted 1st May 2013

DOI: 10.1039/c3an00686g

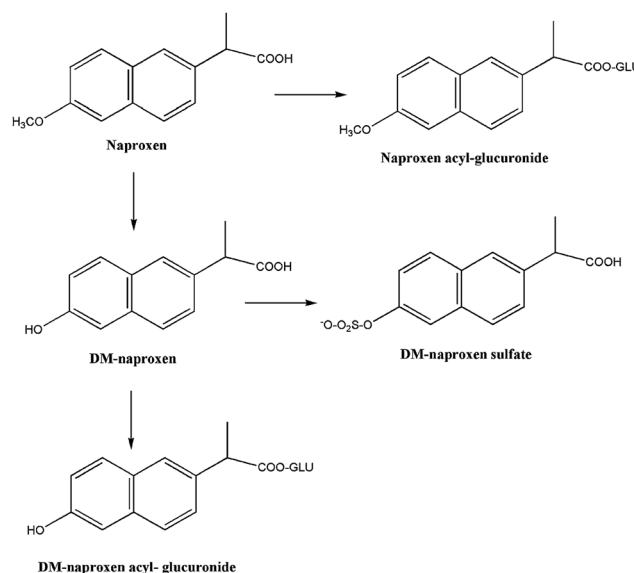
www.rsc.org/analyst

1 Introduction

Naproxen (NAP) belongs to the class of non-steroidal anti-inflammatory drugs (NSAIDs).¹ After oral administration, NAP is partially metabolized to its 6-O-desmethylated metabolite (DM-naproxen); then, both compounds are excreted in urine unchanged or conjugated^{2–4} with glucuronic acid (naproxen and DM-naproxen) or sulfate (DM-naproxen). The metabolic pathways are shown in Scheme 1.⁵

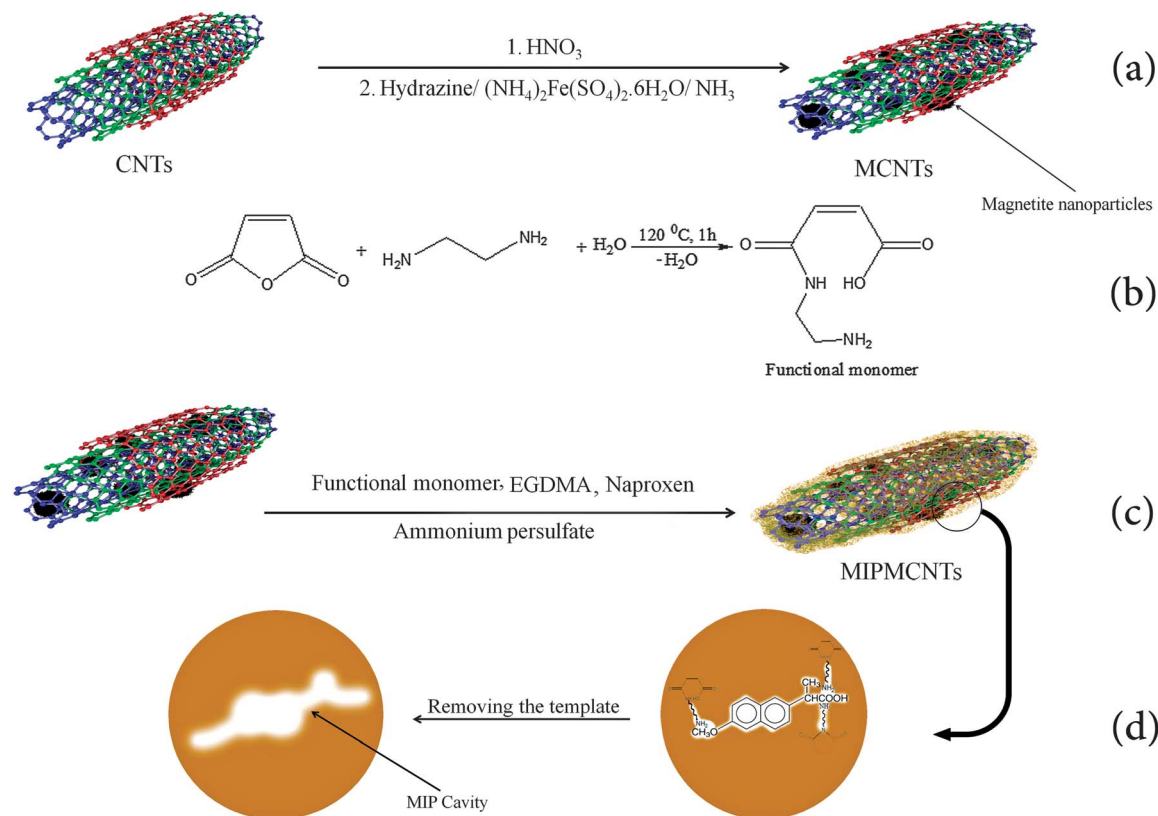
NSAIDs including naproxen are commonly employed to reduce ongoing inflammation, pain and fever, since they are able to block⁶ the cyclo-oxygenase (Cox) enzymes (Cox-1 and Cox-2), that both produce prostaglandins; these classes of compounds have several important functions, as the promotion of inflammation, pain and fever. However, prostaglandins produced by the Cox-1 enzyme are also able to protect the stomach, support platelets and blood clotting. Thus, NSAIDs can cause ulcers in the stomach and promote bleeding after an injury or surgery. Moreover, they are associated with other serious side effects, *i.e.* kidney failure, and with a number of minor side effects, such as nausea, vomiting, diarrhoea, constipation, decreased appetite, rash, dizziness, headache and

drowsiness. When anti-inflammatory treatments become chronic, as in the case rheumatoid arthritis, the patients are exposed to the drugs for prolonged time periods. The potential



Scheme 1 The metabolic pathways of naproxen.

Faculty of Chemistry, Bu Ali Sina University, Hamedan, Iran. E-mail: madrakian@basu.ac.ir; madrakian@gmail.com; Fax: +98-811-8257407; Tel: +98-811-8257407



Scheme 2 Reaction involved in the synthesis of (a) MCNTs, (b) amidoamine monomer, (c) MIPMCNTs and (d) removing the template.

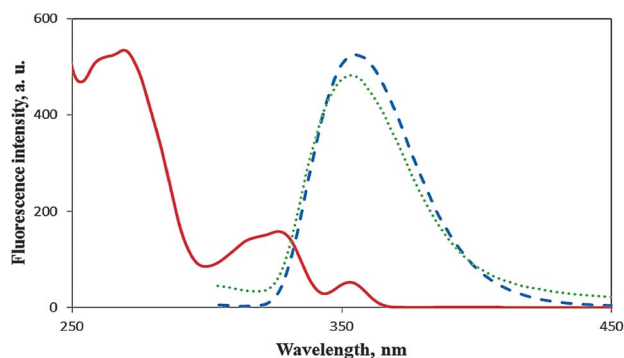


Fig. 1 Fluorescence excitation (—) at 271 nm and emission spectra for NAP in water at pH 3.0 (---) and at pH > 8 (·····) at room temperature.

misuse and involuntary intake of naproxen as residues in food could pose a health risk in people, for example, allergy, severe gastrointestinal lesion, changes in renal function and nephrotoxicity.^{7–9}

In view of the above considerations, the development of a simple and sensitive method for the determination of naproxen in biological fluids could be very useful for toxicological and pharmaceutical purposes. Several methods dealing with naproxen determination in pharmaceutical preparations or biological fluids have been reported, including chemiluminescence,^{10,11} spectrofluorometry,^{12,13} differential pulse voltammetry,¹⁴ gas chromatography-mass spectrometry,¹⁵

electrophoresis¹⁶ and high-performance liquid chromatography (HPLC) with various detection systems.^{17,18} Although these methods have been successfully applied to the analysis of naproxen in various matrices, some of these methods lack sensitivity and suffer from requiring a tedious procedure, being time consuming or involve high cost.

Sample preparation is crucial for obtaining meaningful results from the analysis of real samples, since it is the most tedious and time-consuming step and a possible source of imprecision and inaccuracy of the overall analysis. Solid-phase extraction (SPE) is widely used for the extraction and pre-concentration of analytes in various environmental, food and biological samples. It is the most popular clean-up technique due to factors such as convenience, cost, being time saving and simple, and it is the most accepted sample pretreatment method today.^{19,20} At present, there are several types of sorbents for SPE including normal-phase, reversed-phase, ionic, and other special sorbents. However, due to their unsatisfactory selectivity, these traditional sorbents usually cannot separate analytes efficiently in complex biological or environmental samples.²¹

A relatively new development in the area of SPE is the use of molecularly imprinted polymers (MIPs) for the sample clean-up and development of selective and sensitive analytical methods.^{22–25} MIPs involving the formation of cavities in a synthetic polymer for a template drug are useful for selective extraction. This analytical method is a rapidly developing technique for the preparation polymeric materials that are

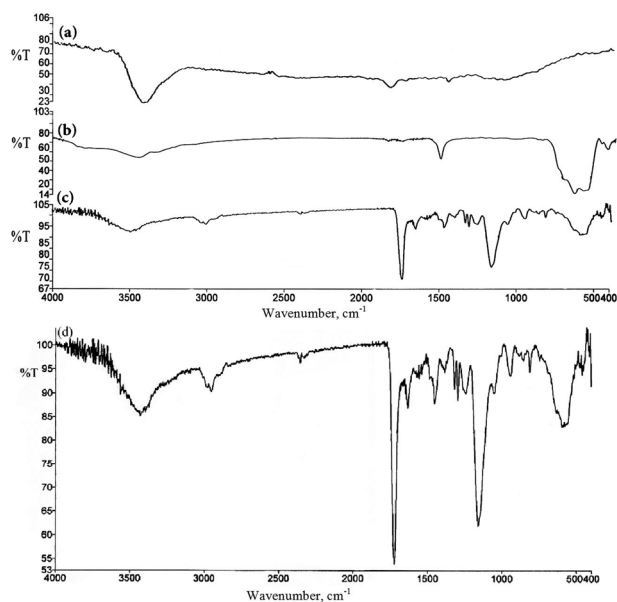


Fig. 2 FT-IR spectra of (a) CNTs, (b) MCNTs, (c) MIPMCNTs and (d) expanded spectrum of (c).

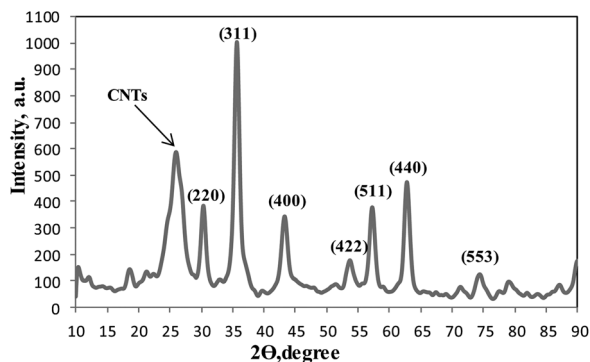


Fig. 3 X-Ray diffraction patterns of MIPMCNTs.

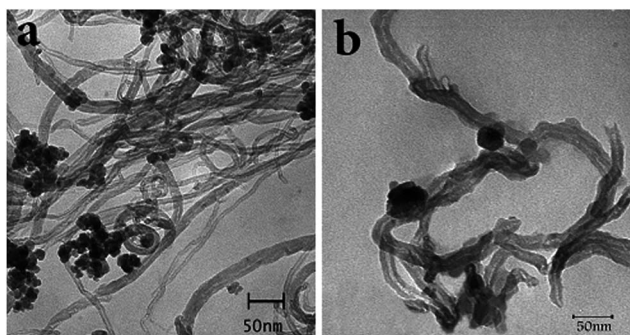


Fig. 4 TEM images of (a) MCNTs and (b) MIPMCNTs.

capable of high molecular recognition.^{26–29} Radical polymerization is usually used for cross-linking of the functional monomers in the presence of template structures before

removal of the target (Scheme 2). Imprinting polymer preparation has generally been based on hydrogen bonding interactions for small compounds. Scientists always try to prepare imprinting polymers with high affinity toward the template compounds. For this purpose the type of monomers and polymerization were designed for better selectivity. The use of MIPs for SPE involves conventional SPE where the MIP is packed into columns or cartridges^{30,31} and batch mode SPE in which the MIP is incubated with the sample.³² A major advantage of MIP-based SPE, related to the high selectivity of the sorbent, is the achievement of an efficient sample clean-up.

In this work, a molecularly imprinted polymer adsorbent is introduced as a solid phase for the selective extraction of NAP from human urine. And then the concentration of NAP in the extract is determined using fluorescence spectroscopy measurement. This procedure is simple, rapid, selective and sensitive. It can be noticed that many works have been published on the determination of naproxen, including, conventional spectrofluorimetry.^{33,34} However, the present method is more rapid, simple and sensitive as compared with previous ones. The developed procedure was then applied to the determination of NAP in urine samples. The determination of naproxen glucuronide was also indirectly performed after chemical hydrolysis of the conjugate.

2 Experimental

2.1 Reagents and materials

All the chemicals used were of analytical reagent grade or the highest purity available from Merck Company (Darmstadt, Germany). Multi-walled carbon nanotubes were purchased from Merck Company (OD, 10–20 nm; length, ~30 μm; SSA, 200 m² g⁻¹). Double distilled water (DDW) was used throughout. All glassware was soaked in dilute nitric acid for 12 h and then thoroughly rinsed with DDW. The NAP stock solution was prepared in methanol and working standard solutions of different NAP concentrations were prepared daily by diluting the stock solution with DDW. Britton–Robinson universal buffer was used for pH adjustment of the working solutions.

2.2 Apparatus

The size, morphology and structure of the nanoparticles were characterized by transmission electronic microscopy (TEM, Philips, CM120, 100 kV). The crystal structure of the synthesized materials was determined using an X-ray diffractometer (XRD, 38066 Riva, d/G. Via M. Misone, 11/D (TN) Italy) at ambient temperature.

A Metrohm model 713 pH-meter was used for pH measurements. A Perkin-Elmer (LS50B) luminescence spectrometer was used for the determination of NAP concentration in solutions. The mid-infrared spectra of multi-walled carbon nanotubes (CNTs), magnetic-modified multi-walled carbon nanotubes (MCNTs) and molecularly imprinted polymer-coated MCNTs (MIPMCNTs) in the region of 4000–400 cm⁻¹ were recorded using an FT-IR spectrometer (Perkin-Elmer model Spectrum

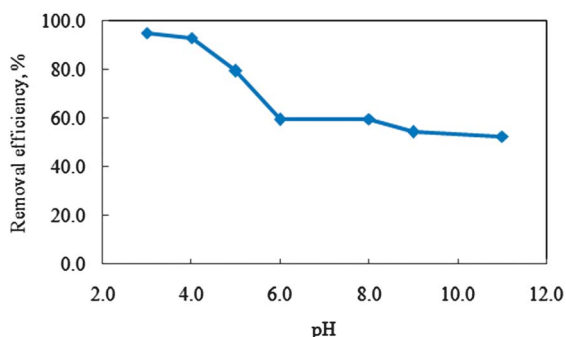


Fig. 5 NAP at different pHs (conditions: 0.02 g of MIPMCNTs, 25 mL of 2.0 mg L^{-1} of NAP, agitation time of 35 min).

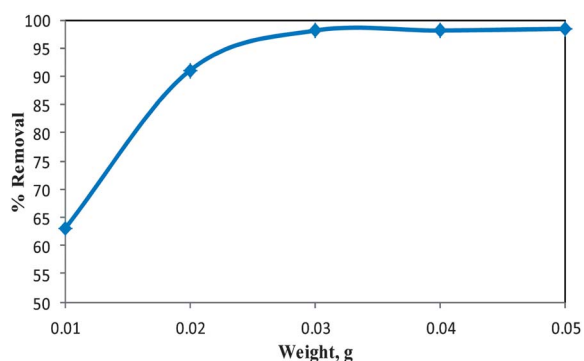


Fig. 6 NAP at different amounts of MIPMCNTs. (conditions: pH 3.0, 25 mL of 2.0 mg L^{-1} of drug, agitation time of 35 min).

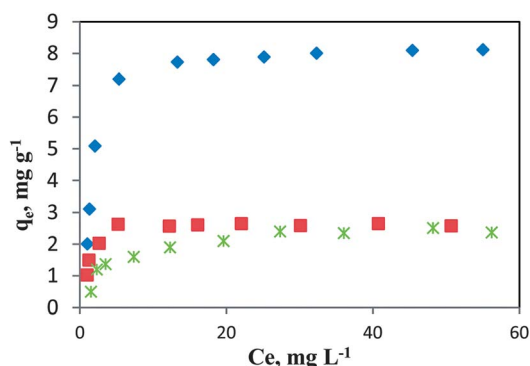


Fig. 7 Isothermal adsorption curves of NAP on MIPMCNTs (◆), NIP (■) and on MCNTs (×) adsorbents.

Table 1 Adsorption isotherm parameters for Langmuir and Freundlich models

Isotherm models Parameters	Langmuir			Freundlich		
	$K_L/L \text{ mg}^{-1}$	$q_m/\text{mg g}^{-1}$	R^2	K_F	$1/n$	R^2
MIPMCNTs	0.46	11.34	0.9987	3.17	0.37	0.8184
NIP	0.86	3.83	0.9971	1.53	0.30	0.7102
MCNTs	0.24	2.63	0.9947	0.72	0.34	0.8067

GX) using KBr pellets. A 40 kHz universal ultrasonic cleaner water bath (RoHS, Korea) was used.

2.3 Preparation of magnetic CNTs (MCNTs)

The magnetic-modified multi-walled carbon nanotubes were achieved according to our previously reported procedure.³⁵ Multi-walled carbon nanotubes were modified using super-magnetic nanoparticles (Scheme 2a).

2.4 Preparation of molecularly imprinted polymer-coated MCNTs (MIPMCNTs) and non-imprinted polymer (NIP)

The amidoamine monomer was synthesized according to a previously reported procedure with some modifications.³⁶ Briefly, the amidoamine monomer was synthesized by the slow addition of 1 g (0.01 mol) maleic anhydride to the solution of 1 mL (0.015 mol) ethylenediamine in 20 mL DDW. The solution was heated at 120°C for 1 h, until all the water was removed and ethylenediamine reacted with maleic anhydride through ring opening (Scheme 2b). In order to prepare the MIPMCNTs, the amidoamine monomer was polymerized in the presence of MCNTs (0.5 g), ammonium persulfate (0.1 g, as the initiator), ethylene glycol dimethacrylate (20 μL , as the cross-linking monomer) and NAP (4 mmol, as the template) in 30 mL DDW at 85°C for 12 h according to Scheme 2c. The product was separated using a magnet and washed with methanol to remove unreacted reagents and then washed overnight with a mixture of methanol/sodium hydroxide aqueous solution (0.1 mol L^{-1}) (9 : 1, v/v) to remove the template. Finally, the product was washed with methanol to neutral pH and the resulting particles were dried under vacuum for 12 h. The NIP nanoparticles were also synthesized by the same procedure, without addition of the template (NAP).

2.5 Preconcentration experiments

To a 25.0 mL sample solution containing NAP and 10.0 mL Britton–Robinson buffer solution of pH 3, 0.03 g of MIPMCNTs was added. The solution was shaken at room temperature for 30 min. Subsequently, the NAP-loaded MIPMCNTs were separated from the mixture with a permanent hand-held magnet within 60 s. The residual amount of the drug in solution was determined spectrofluorometrically at $\lambda_{\text{em}} = 356 \text{ nm}$ ($\lambda_{\text{ex}} = 271 \text{ nm}$) (the emission and excitation spectra of naproxen are shown in Fig. 1). The percent adsorption, *i.e.*, the drug removal efficiency, was determined using the following equation:

$$\%R = \left[\frac{C_0 - C_t}{C_0} \right] \times 100 \quad (1)$$

where C_0 and C_t represent the initial and final (after adsorption) concentrations of the drug in mg L^{-1} , respectively. Also, all the experiments were performed at room temperature.

Adsorption studies for the determination of trace amounts of NAP were performed by adding 100.0 mL of solutions containing $4.0\text{--}40.0 \text{ ng mL}^{-1}$ of NAP and 60 mL of Britton–Robinson buffer of pH 3.0 to 0.03 g of MIPMCNTs and the solutions were stirred for 30 min. The concentration of NAP decreased with time due to adsorption by the MIPMCNTs. The NAP-loaded

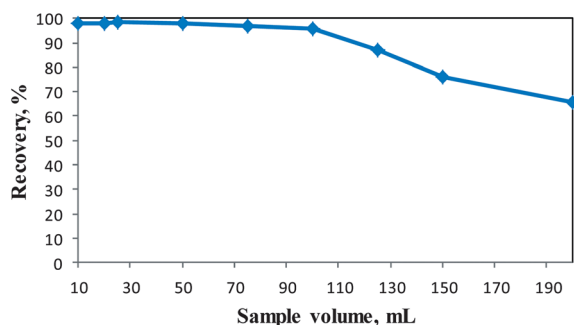


Fig. 8 Effect of initial sample volume (conditions: pH 3.0; contact time, 30 min; MIPMCNTs dosage, 0.02 g).

nanoparticles were separated with magnetic decantation and desorption was performed with 2.0 mL of a 1 : 1 (v/v) mixture of methanol/sodium hydroxide aqueous solution (0.1 mol L^{-1}). The concentration of NAP in the resulting solution was measured spectrofluorometrically at $\lambda_{\text{em}} = 353 \text{ nm}$ ($\lambda_{\text{ex}} = 271 \text{ nm}$) (Fig. 1).

2.6 Point of zero charge of the adsorbent (pH_{PZC})

The point of zero charge (PZC) is a characteristic of metal oxides (hydroxides) and of fundamental importance in surface science. It is a concept relating to the phenomenon of adsorption and describes the condition when the electrical charge density on a surface is zero. The surface charge of MIPMCNTs with carboxyl and amino groups is largely dependent on the pH of the solution, the pH_{PZC} caused by the amphoteric behavior of carboxyl and amino surface groups, and the interaction between surface sites and the electrolyte species. When brought into contact with aqueous solutions, carboxyl groups of surface sites can undergo protonation or deprotonation, depending on the solution pH, to form charged surface species. In this study, the pH_{PZC} of the MIPMCNTs was determined in degassed $0.01 \text{ mol L}^{-1} \text{ NaNO}_3$ solution at 20°C . Aliquots of 30 mL of $0.01 \text{ mol L}^{-1} \text{ NaNO}_3$ were mixed with 30 mg MIPMCNTs in several beakers. The pH of the solutions was adjusted at 4.0, 5.0, 6.0, 7.0, 8.0, 9.0 and 10.0 using HNO_3 and/or NaOH solutions as appropriate. The initial pH values of the solutions were recorded, and the beakers were covered with Parafilm® and shaken for 24 h. The final pH values were recorded and the differences between the initial and the final pH (the so-called ΔpH) of the

solutions were plotted against their initial pH values. The pH_{PZC} corresponds to the pH where $\Delta\text{pH} = 0$.³⁷ pH_{PZC} for MIPMCNTs was determined using the above procedure and was obtained as almost 2.2.

2.7 Urine sample treatment

Drug-free urine samples were collected from healthy donors. Post-dose urine samples were collected from healthy donors who received one dose orally of 220 mg of naproxen. All urine samples were stored at -20°C . Then, 40.0 mL of each sample was diluted with 60 mL of Britton–Robinson buffer of pH 3.0 solution and directly subjected to the SPE procedure. Urine samples were spiked with NAP at 10 and 20 ng mL^{-1} concentration levels. Acid hydrolysis was performed on post-dose urine samples. All experiments were performed in compliance with the relevant laws and institutional guidelines, and Behbood institute (Hamedan, Iran) has approved the experiments.

Acid hydrolysis. A 0.5 mL aliquot of 37% HCl solution was added to 1.0 mL of urine, and incubated at 56°C for 90 min. Then, the solution was diluted 1 : 1 with NaOH (2 mol L^{-1}). Finally, 50 μL of the resulting mixture was diluted and analyzed as previously described.

3 Results and discussion

3.1 Characterization of the adsorbent

The FTIR spectra of the products in each step of the MIPMCNTs synthesis were recorded to verify the formation of the expected products. The related spectra are shown in Fig. 2. The characteristic absorption band of Fe–O in Fe_3O_4 (around 580 cm^{-1}) was observed in Fig. 2b. This confirms that the CNTs were modified with magnetite nanoparticles. Two new absorption peaks at 1729.3 cm^{-1} and 1440 cm^{-1} in Fig. 2c are assigned to C=O and C–N bands in the polymer-coated final product (MIPMCNTs). Moreover, new absorption peaks at 3248.6 and 3071.9 cm^{-1} are related to the stretching modes of the amino group (N–H) (observable in Fig. 2d).³⁸ Based on the above results, it can be concluded that the fabrication procedure (in Section 2.4) has been successfully performed.

The XRD pattern (Fig. 3) shows diffraction peaks that are indexed to the (2 2 0), (3 1 1), (4 0 0), (4 2 2), (5 1 1), (4 4 0) and (5 5 3) reflection characteristics of the cubic spinel phase of Fe_3O_4 (JCPDS powder diffraction data file no. 79-0418), revealing that the resultant MIPMCNTs were modified with

Table 2 Assay of NAP in human urine samples by means of the proposed method ($n = 5$)

Sample	Spiked value/ ng mL^{-1}	Found/ ng mL^{-1}			Recovery percentage (%)			Deconjugation acid hydrolysis/ ng mL^{-1}		
		MCNTs	NIP	MIPMCNTs	MCNTs	NIP	MIPMCNTs	MCNTs	NIP	MIPMCNTs
Human urine	—	0.00 ± 0.02	0.00 ± 0.01	0.00 ± 0.01	—	—	—	—	—	—
	10	9.23 ± 0.01	9.58 ± 0.01	9.77 ± 0.01	92.3	95.8	97.7	—	—	—
	20	18.70 ± 0.02	19.46 ± 0.02	19.88 ± 0.01	93.5	97.3	99.4	—	—	—
Infected human urine	—	56.21 ± 2.13	100.20 ± 1.53	162.11 ± 1.03	—	—	—	94.62 ± 0.10	120.22 ± 0.18	238.81 ± 0.09
	10	58.32 ± 1.46	105.22 ± 0.88	171.76 ± 0.98	21.1	50.2	96.5	96.21 ± 0.12	128.20 ± 0.09	247.02 ± 0.07
	20	61.33 ± 1.30	115.41 ± 1.51	182.55 ± 0.87	25.0	76.0	102.2	100.24 ± 0.08	138.45 ± 1.21	260.11 ± 0.05

Table 3 Comparison of the proposed method with other reported methods for NAP determination^a

Method	LOD/ng mL ⁻¹	Linear range/ng mL ⁻¹	Reference
FL ^b	20	200–2000	42
MECC–LIF	70	100–2000	15
SPE–HPLC–UV	30	200–20000	5
SPE–HPLC–FL	—	8–96	18
HPLC–ECL	16	40–2000	6
MIP–SPE–FL	2	4–40	This method

^a MECC: micellar electrokinetic capillary chromatography. LIF: laser-induced fluorescence. SPE: solid-phase extraction. ECL: electrogenerated chemiluminescence. ^b Spectrofluorometric determination in basic medium.

magnetite nanoparticles. Furthermore the typical peaks of CNTs at $2\theta = 25.91^\circ$ can be observed. The average crystallite size of the Fe₃O₄ nanoparticles was estimated to be 16 nm from the XRD data according to the Scherrer equation.³⁵

The TEM images of the MCNTs and MIPMCNTs are shown in Fig. 4a and ab. Fig. 4a indicates that the CNTs were modified with magnetite nanoparticles and Fig. 4b indicates that the MCNTs were almost coated with a thin layer of polymer and contain magnetite nanoparticles.

3.2 Effect of solution pH on NAP uptake

Solution pH affects the adsorption process of drug molecules by affecting both the aqueous chemistry and surface binding-sites of the adsorbent. The effect of pH on the NAP removal was investigated in the range of 3.0–11.0 using an initial NAP concentration of 2.0 mg L⁻¹ and a stirring time of 35 min, where the pH was adjusted with Britton–Robinson buffer. Fig. 5 indicates that the adsorbent provides the highest affinity for NAP at pH 3.0. This is reasonable, because the adsorbent at pH 3 is negatively charged and the analyte is protonated at this pH (pH_{PZC} of MIPMCNTs is 2.2 and pK_a of NAP is 4.2³⁹), and hence, the highest electrostatic interaction between NAP and MIPMCNTs is expected at this pH.

3.3 Effect of adsorbent dosage on the drug adsorption

The dependence of the adsorption of the drug on the amount of modified nanoparticles was studied at room temperature and at pH 3.0 by varying the adsorbent amount from 0.01 to 0.05 g in contact with 25 mL solution of 2.0 mg L⁻¹ of NAP. The results are shown in Fig. 6. Apparently, the percentage removal of NAP increased with increasing amount of MIPMCNTs due to the availability of a higher number of adsorption sites. The adsorption reached a maximum with 0.03 g of adsorbent, at which the maximum percentage removal was about 98%.

3.4 Effect of contact time

The effect of contact time on the adsorption of the drug was studied to determine the time needed to remove NAP by MIPMCNTs from a 2.0 mg L⁻¹ solution of the drug at pH 3.0. A 0.03 g aliquot of the adsorbent was added into 25 mL (containing 10.0 mL of buffer solution of pH 3) of the drug solution.

The fluorescence intensity of NAP was monitored *versus* time to determine the variation of the drug concentration. It was observed that after a contact time of about 30.0 min, almost all the drug was adsorbed.

3.5 Adsorption isotherms

The capacity of the adsorbent is an important factor that determines how much sorbent is required to quantitatively remove a specific amount of the drug from solution. For measuring the adsorption capacity of the MIPMCNTs, the adsorbent was added into NAP solutions at various concentrations, and the suspensions were stirred at room temperature, followed by magnetic removal of the adsorbent. An adsorption isotherm describes the fraction of the sorbate molecules that are partitioned between the liquid and the solid phase at equilibrium. Adsorption of the drug by MIPMCNTs, NIP and MCNTs adsorbents was modelled using Freundlich⁴⁰ and Langmuir⁴¹ adsorption isotherms. The NAP remaining in the supernatants was measured spectrofluorometrically at $\lambda_{em} = 356$ nm ($\lambda_{ex} = 271$ nm), and the results were used to plot the isothermal adsorption curves as shown in Fig. 7. The equilibrium adsorption data were fitted to Langmuir and Freundlich isotherm models by linear regression. The resulting parameters are summarized in Table 1.

The higher correlation coefficient obtained for the Langmuir model ($R^2 > 0.99$) indicates that the experimental data are better fitted into this model, and that the adsorption of NAP on MIPMCNTs is more compatible with Langmuir assumptions, *i.e.*, adsorption takes place at specific homogeneous sites within the adsorbent. The Langmuir model is based on the physical hypothesis that the maximum adsorption capacity consists of a monolayer adsorption, that there are no interactions between adsorbed molecules, and that the adsorption energy is distributed homogeneously over the entire coverage surface. This sorption model serves to estimate the maximum uptake values where they cannot be reached in the experiments.

According to the results (Table 1), the maximum amount of NAP that can be adsorbed by MIPMCNTs was found to be 11.34 mg g⁻¹ at pH 3.0. The relatively high adsorption capacity of MIPMCNTs in comparison with NIP and MCNTs shows that the adsorption of NAP molecules takes place at a large number of specific homogeneous sites within the adsorbent (specific cavities of the MIP), besides non-specific interactions which are approximately identical for both MIPMCNTs and NIP adsorbents.

3.6 Reusability and stability

The reusability and stability of MIPMCNTs for the extraction of NAP was assessed by performing five consecutive separations–desorption cycles under the optimized conditions (0.03 g of MIPMCNTs, 25 mL of 2.0 mg L⁻¹ of NAP, agitation time of 30 min). The desorption of NAP from the adsorbent was performed with a mixture of methanol/sodium hydroxide aqueous solution (0.1 mol L⁻¹) as described in Section 2.5. There was no significant change in the performance of the adsorbent during these cycles, indicating that the fabricated MIPMCNTs are a

reusable and stable solid phase sorbent for the extraction of NAP.

3.7 Effect of sample volume

The effect of sample volume on the drug adsorption was studied in the range 10.0–200.0 mL; 10.0 mL samples containing 2.0 mg L^{-1} of the drug were diluted to 10.0, 20.0, 25.0, 50.0, 75.0, 100.0, 125.0, 150.0 and 200.0 mL with DDW. Then adsorption and desorption processes were performed under the optimum conditions (pH 3.0; contact time, 30 min; MIPMCNTs dosage, 0.02 g) as described in the Experimental section. The results showed (Fig. 8) that the drug content in the volumes up to 100.0 mL was completely and quantitatively adsorbed by the nanoparticles, but there was a decrease in the amount adsorbed at higher volumes. Therefore, for the determination of trace quantities of the drug, a sample volume of 100.0 mL was selected for a high preconcentration factor.

3.8 Analytical parameters and applications

A calibration graph was constructed from spectrofluorometric measurements of the desorbed NAP after performing the adsorption/separation under the optimum conditions as described above. The calibration graph was linear in the range of $4.0\text{--}40.0 \text{ ng mL}^{-1}$ for a sample volume of 100.0 mL. The calibration equation is $IF = 24.34C + 14.53$ with a determination coefficient of 0.9991 ($n = 10$), where IF is the fluorescence intensity of the eluate at $\lambda_{\text{em}} = 353 \text{ nm}$ ($\lambda_{\text{ex}} = 271 \text{ nm}$) and C is the concentration of the drug in ng mL^{-1} . The limit of detection, defined as $LOD = 3S_b/m$, where LOD, S_b and m are the limit of detection, standard deviation of the blank and the slope of the calibration graph, respectively, was 2.0 ng mL^{-1} of NAP. As the drug in 100.0 mL of the sample solution was concentrated into 2.0 mL, a maximum preconcentration factor of 50.0 was achieved in this method.

The analytical applicability of the proposed method was evaluated by determining the NAP content of infected and healthy human urine samples using MCNTs, NIP and MIPMCNTs adsorbents. The samples were also analyzed after spiking with different amounts of the drug. The relative standard deviations (RSDs) for 5.0 and 30.0 ng mL^{-1} of the drug (in the case of MIPMCNTs) were 0.95% and 0.36% ($n = 5$), respectively. The results given in Table 2 show good recoveries of the proposed method for the NAP added to urine samples in the case of MCNTs, NIP and MIPMCNTs adsorbents. But in the case of infected human urine, good recoveries were achieved only in the case of MIPMCNTs. These results are probably due to presence of naproxen glucuronide, at a higher concentration level than naproxen, and the non-selective tendency of MCNTs and the NIP adsorbents to naproxen and its conjugated form. In fact, naproxen glucuronide has no interference in the selective extraction of naproxen in the case of the MIPMCNTs adsorbent.

Acid hydrolysis was then independently performed as described in the Experimental section in order to indirectly determinate the amount of naproxen glucuronide as a measurement of the difference for the parent drug before and after the hydrolysis. The naproxen glucuronide concentration

estimated, using the MIPMCNTs adsorbent, after acid hydrolysis was almost 76.51 ng mL^{-1} .

Table 3 shows a comparison between the results obtained by the present method with those obtained by some other methods reported for the determination of NAP. As compared in Table 3, the present method has a lower detection limit and the lowest linear range compared with HPLC and pure spectrofluorometric methods for determination of NAP. It should be highlighted that the major advantages of the magnetic separation with MIPMCNTs are easy separation and the reversibility of the process, *i.e.*, the adsorbent is easily attracted by a magnet and can be separated from the liquid medium, the drug can be recovered from the adsorbent and the regenerated adsorbent can be reused for further drug removal experiments.

4 Conclusions

A selective naproxen-imprinted polymer was prepared by suspension polymerization. The preparation of this material was relatively simple and rapid. This study indicated that the sorption of naproxen onto the imprinted polymer was much better than the non-imprinted polymer. The imprinted polymer also presents an advantage of a high adsorption capacity and high chemical stability. Furthermore, the adsorbent is easily attracted using a magnet and can be separated from the liquid medium, which enables an easy separation process. Based on the Langmuir isotherm analysis, the adsorption capacity was about 11.34 mg g^{-1} . The imprinted polymer-solid-phase extraction was successfully applied to the analysis of naproxen in the human urine samples.

References

- 1 C. Boynton, C. Dick and G. Mayer, *J. Clin. Pharmacol.*, 1988, **28**, 512.
- 2 G. F. Thompson and J. M. Collins, *J. Pharm. Sci.*, 1973, **62**, 937.
- 3 Y. Sugawara, M. Fujihara, Y. Miura, K. Hayashida and T. Takahashi, *Chem. Pharm. Bull.*, 1978, **26**, 3312.
- 4 C. H. Kiang, C. Lee and S. Kushinsky, *Drug Metab. Dispos.*, 1989, **17**, 43.
- 5 A. Aresta, F. Palmisano and C. G. Zambonin, *J. Pharm. Biomed. Anal.*, 2005, **39**, 643.
- 6 Y. Sun, Z. Zhang, Z. Xi and Z. Shi, *Talanta*, 2009, **79**, 676.
- 7 G. Singh and G. Triadafilopoulos, *J. Rheumatol.*, 1999, **26**, 18.
- 8 I. F. Fries, *N. Engl. J. Med.*, 1999, **341**, 1397.
- 9 L. Kovacevic, J. Bernstein, R. P. Valentini, A. Imam, N. Gupta and T. K. Mattoo, *Pediatr. Nephrol.*, 2003, **18**, 826.
- 10 X. L. Cheng, L. X. Zhao, M. L. Liu and J. M. Lin, *Anal. Chim. Acta*, 2006, **558**, 296.
- 11 Y. H. Li and J. R. Lu, *Anal. Chim. Acta*, 2006, **577**, 107.
- 12 E. P. Zisiou, P. C. A. G. Pinto, M. L. M. F. S. Saraiva, C. Siquet and J. L. F. C. Lima, *Talanta*, 2005, **68**, 226.
- 13 G. A. Ibáñez and G. M. Escandar, *J. Pharm. Biomed. Anal.*, 2005, **37**, 149.
- 14 N. Adhouma, L. Monser, M. Toumi and K. Boujlel, *Anal. Chim. Acta*, 2003, **495**, 69.

- 15 Á. Sebők, A. Vasanits-Zsigrai, G. Palkó, G. Záray and I. Molnár-Perl, *Talanta*, 2008, **76**, 642.
- 16 C. Albrecht and W. Thormann, *J. Chromatogr., A*, 1998, **802**, 115.
- 17 P. Mishra, S. Arif and A. K. Shakya, *J. Inst. Chem.*, 1993, **65**, 27.
- 18 E. Mikami, T. Goto, T. Ohno, H. Matsumoto and M. Nishida, *J. Pharm. Biomed. Anal.*, 2000, **23**, 917.
- 19 M. Javanbakht, A. M. Attaran, M. H. Namjumanesh, M. Esfandiyari-Manesh and B. Akbari-adegani, *J. Chromatogr., B: Anal. Technol. Biomed. Life Sci.*, 2010, **878**, 1700.
- 20 M.-C. Hennion, *J. Chromatogr., A*, 1999, **856**, 3.
- 21 C. He, Y. Long, J. Pan, K. Li and F. Liu, *J. Biochem. Biophys. Methods*, 2007, **70**, 133.
- 22 *Molecularly Imprinted Polymers: Man-Made Mimics of Antibodies and their Applications in Analytical Chemistry (Techniques and Instrumentation in Analytical Chemistry)*, ed. B. Sellergren, Elsevier, Amsterdam, 2001, vol. 23.
- 23 Y. Li, X. Li, J. Chu, C. Dong, J. Qi and Y. Yuan, *Environ. Pollut.*, 2010, **158**, 2317.
- 24 Z. Lin, W. Cheng, Y. Li, Z. Liu, X. Chen and C. Huang, *Anal. Chim. Acta*, 2012, **720**, 71.
- 25 N. Masque, R. M. Marce and F. Borrull, *TrAC, Trends Anal. Chem.*, 2001, **20**, 477.
- 26 S. Rimmer, *Chromatographia*, 2008, **67**, 343.
- 27 D. Wang, S. Pyo Hong, G. Yang and K. Ho Row, *Korean J. Chem. Eng.*, 2003, **20**, 1073.
- 28 I. A. Nicholls and J. P. Rosengren, *Bioseparation*, 2002, **10**, 301.
- 29 S. G. Dmitrienko, V. V. Irkha, A. Y. Kuznetsova and Y. A. Zolotov, *J. Anal. Chem.*, 2004, **59**, 808.
- 30 M. Walshe, J. Howarth, M. T. Kelly, R. O'Kennedy and M. R. Smyth, *J. Pharm. Biomed. Anal.*, 1997, **16**, 319.
- 31 A. Zander, P. Findlay, T. Renner, B. Sellergren and A. Swietlow, *Anal. Chem.*, 1998, **70**, 3304.
- 32 L. I. Andersson, A. Paprica and T. Arvidsson, *Chromatographia*, 1997, **46**, 57.
- 33 I. Velar, M. Sanchez, A. Zornoza and N. Goyenechea, *Biomed. Chromatogr.*, 1999, **13**, 155.
- 34 D. Wu, *Yaowu Fenxi Zazhi*, 1999, **19**, 62.
- 35 T. Madrakian, A. Afkhami, M. Ahmadi and H. Bagheri, *J. Hazard. Mater.*, 2011, **196**, 109.
- 36 N. M. Mahmoodi, F. Najafi and A. Neshat, *Ind. Crops Prod.*, 2013, **42**, 119.
- 37 H. Bagheri, A. Afkhami, M. S. Tehrani and H. Khoshshafar, *Talanta*, 2012, **97**, 87.
- 38 T. Madrakian, A. Afkhami, M. A. Zolfigol, M. Ahmadi and N. Koukabi, *Nano-Micro Lett.*, 2012, **4**, 57.
- 39 Y. L. Xu, Z. S. Liu, H. F. Wang, C. Yan and R. Y. Gao, *Electrophoresis*, 2005, **26**, 804.
- 40 H. Freundlich and W. Heller, *J. Am. Chem. Soc.*, 1939, **61**, 2228.
- 41 I. Langmuir, *J. Am. Chem. Soc.*, 1916, **38**, 2221.
- 42 P. Damiani, M. Bearzotti and M. A. Cabezón, *J. Pharm. Biomed. Anal.*, 2002, **29**, 229.